JEE Journal of Ecological Engineering

Journal of Ecological Engineering, 2026, 27(9), 57–66
https://doi.org/10.12911/22998993/220703
ISSN 2299–8993, License CC-BY 4.0

Received: 2026.01.02
Accepted: 2026.07.15
Published: 2026.08.01

Eco-engineered iron(II,III) oxide/activated carbon composites from *Arenga pinnata* palm fiber for structures, microwave absorption and dielectric properties

Martha Rianna[1*], Herty Afrina Sianturi[1], Marnala Windawati Togatorop[1], Timbangen Sembiring[1], Anggito P. Tetuko[2], Eko Arief Setiadi[2], Nanang Sudrajat[3], Akrajas Ali Umar[4]

[1] Universitas Sumatera Utara, Medan, 20155, Indonesia
[2] Research Center for Advanced Materials, National Research and Innovation Agency (BRIN), Tangerang Selatan, Banten, 15314, Indonesia
[3] Research Center for Electronics, National Research and Innovation Agency Republic of Indonesia (BRIN), Bandung, Jawa Barat, 40135, Indonesia
[4] Institute of Microengineering and Nanoelectronics (IMEN), Universiti Kebangsaan Malaysia, UKM, Bangi, Selangor, 43600, Malaysia
* Corresponding author's email: marthariana@usu.ac.id

ABSTRACT

This study reports the synthesis and characterization of sustainable activated carbon–based composites derived from Arenga pinnata palm fiber and natural iron sand for X-band microwave absorption. The composites were prepared via a coprecipitation-assisted route using palm fiber–derived carbon and natural iron sand at mass ratios of 1:1, 3:5, and 5:3. Structural, morphological, and electromagnetic properties were evaluated using X-ray diffraction (XRD), scanning electron microscopy–energy dispersive X-ray spectroscopy (SEM-EDX), and vector network analysis (VNA) in the 8–12 GHz range. XRD confirmed the formation of a dominant cubic spinel Fe_3O_4 phase with an amorphous carbon matrix, while SEM-EDX revealed porous morphologies with homogeneously distributed C, Fe, and O. The average particle sizes ranged from 0.207 to 0.241 μm. Microwave absorption measurements showed effective attenuation for all compositions, with the 3:5 composite achieving the best performance, exhibiting a minimum reflection loss of −12.31 dB at 10.54 GHz and an absorption efficiency of 87%. The enhanced absorption is attributed to the synergistic interaction between magnetic and dielectric loss mechanisms.

Keywords: Fe_3O_4/C, activated carbon fiber, natural iron sand, dielectric.

INTRODUCTION

Human exposure to electromagnetic radiation, particularly in the microwave frequency range, has increased significantly due to rapid advances in communication systems and electronic technologies (Salford et al., 2003). Excessive electromagnetic radiation has been associated with potential adverse health effects, which has intensified global efforts to develop effective strategies for mitigating electromagnetic pollution, especially through absorption-based materials (Pattanayak et al., 2021). Microwave absorbing materials are typically engineered by integrating magnetic and conductive components to efficiently attenuate incident electromagnetic waves (Al-Mattarneh, 2018).

Indonesia possesses abundant natural iron sand resources, which are widely distributed in coastal and riverine regions (Rianna et al., 2023, 2025). Natural iron sand commonly contains magnetite (Fe_3O_4) as the dominant phase, along with minor amounts of hematite (α-Fe_2O_3) and maghemite (γ-Fe_2O_3) (Rianna et al., 2019). In recent years, considerable research efforts have been devoted to developing advanced microwave absorbers using innovative material systems and fabrication techniques (K. Li et al., 2025). Various absorber materials, including ferrites, ceramics, and carbon-based materials, have been investigated to meet the increasing demand for lightweight, efficient, and broadband absorbers (Elmahaishi et al., 2022).

Microwave absorbers are generally classified into dielectric loss–based and magnetic loss–based materials. Dielectric absorbers typically exhibit high permittivity but suffer from poor impedance matching due to the absence of magnetic response. Consequently, combining dielectric and magnetic components has emerged as an effective strategy to enhance impedance matching and absorption efficiency (W. Li et al., 2024). Among conventional absorber materials, ferrites are particularly attractive because of their strong magnetic loss mechanisms and favorable impedance matching, which enable efficient microwave attenuation at low to intermediate frequencies (Chen et al., 2025). In particular, Fe_3O_4 (magnetite) has gained significant attention due to its high magnetic permeability, strong interaction with electromagnetic fields, chemical stability, and resistance to oxidation compared with metallic absorbers (Houbi et al., 2021; X. Zhou et al., 2019). Fe_3O_4-based materials have been reported to exhibit high reflection loss values and wide effective absorption bandwidths, depending on their composition and microstructure (Zhang et al., 2019; J. Zhou et al., 2025). Numerous studies have demonstrated that Fe_3O_4-based composites can achieve reflection loss values below −10 dB, even at relatively thin thicknesses (Fionov et al., 2022). For example, Yin et al. reported that Fe_3O_4 crystals used in microwave absorbers exhibited effective absorption in the 2–15 GHz range with a reflection loss of −10.5 dB at 10.4 GHz (P. Yin et al., 2018).

Carbon-based materials have also attracted increasing interest for microwave absorption applications due to their low density, good chemical stability, large surface area, high electrical conductivity, and tunable dielectric properties (Chitraningrum et al., 2022, 2024; Kaur and Aul, 2014). Carbon materials enable the fabrication of thin, lightweight, and flexible absorbers with broad absorption bandwidths and excellent environmental resistance (Liu et al., 2023). *Arenga pinnata* (aren) is a palm species that produces coarse black fibers, commonly known as palm fiber or ijuk (Imraan et al., 2023). Due to its high lignin (31.5–43.9%) and cellulose (50.5–52.3%) content, palm fiber is considered a promising biomass precursor for carbon production (Meng et al., 2019). Previous studies have shown that palm fiber–derived carbon exhibits strong attenuation properties and multifunctional absorption capabilities (Adrianto et al., 2019; Sitepu et al., 2019).

Recent investigations have demonstrated that combining carbon and ferrite phases in composite systems significantly enhances microwave absorption performance, often achieving reflection loss values below −10 dB in the X-band frequency range (Mahmoodi et al., 2022). The absorption performance of such composites is strongly influenced by synthesis methods, compositional ratios, and microstructural characteristics (Izaak et al., 2021; Z. Yin et al., 2016). Notably, carbon–ferrite composites have been reported to achieve reflection loss values as low as −28 dB at 10.2 GHz, highlighting the advantage of synergistic magnetic–dielectric interactions (Dipak et al., 2019; Q. Sun et al., 2018).

In this study, activated carbon derived from Arenga pinnata palm fiber and natural iron sand was synthesized to develop a sustainable Fe_3O_4/carbon composite for microwave absorption applications. The novelty of this work lies in the direct valorization of locally abundant Arenga pinnata palm fiber and natural Indonesian iron sand into an eco-engineered Fe_3O_4/activated carbon microwave absorber without the use of synthetic ferrite precursors. Unlike many previously reported Fe_3O_4/carbon systems that rely on chemically synthesized nanoparticles or fossil-derived carbon sources, this study employs biomass-derived activated carbon and naturally occurring magnetite, offering a sustainable and low-cost material pathway. In addition, this work provides a systematic correlation between composition ratio, microstructure, electromagnetic parameters (μ and ε), and X-band reflection loss, revealing the role of magnetic–dielectric synergy and impedance matching in achieving effective absorption (RL < −10 dB) (Negi et al., 2022). The findings demonstrate that an optimized balance between natural Fe_3O_4 and biomass-derived carbon can deliver stable and efficient microwave attenuation, highlighting the potential of this composite system for environmentally friendly electromagnetic interference mitigation. The structural, morphological, and electromagnetic properties of the composites were systematically investigated using X-ray diffraction

(XRD), scanning electron microscopy–energy dispersive X-ray spectroscopy (SEM–EDX), and vector network analysis (VNA). XRD was employed to identify crystalline phases and structural parameters (Allahkarami et al., 2022; Sivaprakash et al., 2017), while SEM–EDX was used to examine surface morphology and elemental distribution (Ye et al., 2018). Microwave absorption behavior, including complex permittivity (ε′–jε″) and permeability (μ′–jμ″), was evaluated using VNA measurements in the X-band (Ghigna et al., 2020; Teber et al., 2018). The results provide insight into the structure–property relationships governing microwave attenuation and highlight the potential of biomass-derived Fe_3O_4/carbon composites as efficient and environmentally friendly microwave absorbers.

METHODS

Preparation of activated carbon

The palm fiber (*Arenga pinnata*, locally known as ijuk) was first washed thoroughly with running water to remove impurities and then cut into small pieces to facilitate the carbonization process. The cleaned fibers were carbonized in a furnace at 500 °C for 1 h to obtain ijuk-derived carbon. Subsequently, the carbonized material was chemically activated by immersion in 150 mL of a 30% NaCl solution under continuous stirring at 500 rpm and 80 °C for 2.5 h. After the activation process, the suspension was allowed to settle and then filtered. The resulting carbon was repeatedly washed with distilled water to remove residual activating agents, yielding activated carbon powder derived from palm fiber.

Preparation of natural iron sand

Natural iron sand was collected from a river in Jangga Toruan Village, Lumban Julu Subdistrict, using a bar magnet to enrich the magnetic fraction. The collected iron sand was sieved through a 100-mesh sieve to obtain uniform particle sizes. The sieved material was then washed sequentially with distilled water and 70% ethanol to remove impurities. After washing, the suspension was allowed to settle for 30 min, followed by filtration. The purified iron sand was dried in an oven at 200 °C for 1 h, allowed to cool to room temperature overnight, and subsequently ground to obtain fine iron sand powder.

Synthesis of activated "*Arenga Pinnata*" palm fiber and natural iron sand

The two raw materials, activated carbon and natural iron sand, were first ground and sieved through a 100-mesh sieve to ensure uniform particle size. The powders were then mixed at a mass ratio of 3:1 and processed using a high-energy milling (HEM) technique at a rotational speed of 500 rpm for 1 h. This milling process was conducted to achieve homogeneous mixing and particle size refinement, thereby increasing the effective surface area of the activated carbon and enhancing interfacial contact between the carbon and iron sand phases. Subsequently, the milled mixture was calcined in a furnace at 1000 °C for 1 h. After calcination, the resulting solid was allowed to cool to room temperature and then ground into a fine powder for further characterization.

Characterization

X-ray diffraction (XRD) was employed to examine the crystalline phases, microstructure, and lattice parameters of the activated carbon and natural iron sand composites. Scanning electron microscopy coupled with energy-dispersive X-ray spectroscopy (SEM-EDX) was used to investigate the surface morphology and elemental distribution of the samples. Microwave absorption properties were evaluated using a vector network analyzer (VNA) in the X-band frequency range.

RESULTS AND DISCUSSION

XRF analysis of carbon fiber and natural iron sand

X-ray fluorescence (XRF) analysis was conducted to determine the elemental composition of the raw materials, namely *Arenga pinnata*–derived carbon fiber and natural iron sand. The results revealed that the natural iron sand contained a high iron (Fe) content of 49.52%, confirming its suitability as the primary source of the magnetic Fe_3O_4 phase responsible for magnetic loss mechanisms in microwave absorption. Minor elements such as Al, Si, Ti, and Mg were also detected at lower concentrations and may contribute to interfacial polarization effects.

In contrast, the *Arenga pinnata* carbon fiber was dominated by Ca (28.27%), Mg (18.20%), and Si (9.69%), with only a small Fe content (0.54%). The low iron concentration indicates a negligible contribution to magnetic loss; however, the presence of these non-magnetic elements within the carbon matrix enhances dielectric loss through dipolar polarization and interfacial polarization mechanisms. In addition, the carbon-rich structure promotes electrical conductivity, which contributes to conduction loss and facilitates effective impedance matching. The complementary roles of the magnetic Fe_3O_4 phase and the dielectric carbon matrix are therefore critical in achieving efficient microwave attenuation in the composite system (Ramadani and Zakir, 2025).

XRD analysis of the Fe_3O_4/C

X-ray diffraction (XRD) analysis was performed to examine the phase composition, crystal structure, and crystallinity of the Fe_3O_4/activated carbon composites derived from natural iron sand and Arenga pinnata palm fiber. All composition variants exhibited similar diffraction features, with dominant peaks at approximately 31.5°, 35.1°, 40.1°, and 44.6°, corresponding to the (220), (311), (110), and (400) planes of cubic spinel magnetite (Fe_3O_4). These reflections confirm the successful formation of the Fe_3O_4 phase without detectable secondary iron oxide impurities, consistent with previously reported Fe_3O_4/carbon-based microwave absorbers (Mohammadifard et al., 2022).

Broad, low-intensity diffraction features in the 15°–27° range indicate the presence of an amorphous carbon phase originating from the biomass-derived activated carbon, which is characteristic of sustainable Fe_3O_4/C systems reported in the literature (Yang et al., 2016; Yusmadi et al., 2025). The coexistence of crystalline Fe_3O_4 and amorphous carbon is known to promote synergistic magnetic–dielectric interactions and improved impedance matching (Pakniyakan and Aslibeiki, 2024).

The calculated crystallite sizes were 26.31 nm (1:1), 27.77 nm (3:5), and 26.10 nm (5:3), falling within the range commonly reported for Fe_3O_4/C composites exhibiting effective X-band microwave absorption. The highest crystallinity (78%) was observed for the 5:3 composite due to its higher iron sand content, while the lowest crystallinity (65%) occurred for the carbon-rich 3:5 composite. The balanced 1:1 composite exhibited intermediate crystallinity (74%). These results demonstrate that increasing carbon content suppresses crystallinity by enhancing the amorphous phase, a trend widely reported in Fe_3O_4/carbon absorber systems and favorable for dielectric loss enhancement (Figure 1, Table 1) (Suresha et al., 2025)(Luo et al., 2019).

The relative intensity of the Fe_3O_4 diffraction peaks increases with increasing iron sand content, with the 5:3 composite showing the sharpest and most intense peaks, indicating a higher degree of crystallinity. In contrast, the 3:5 composite, which contains a higher proportion of activated carbon, exhibits reduced peak intensity and broader diffraction features, reflecting the suppression of crystallinity by the amorphous carbon phase. A broad diffuse hump observed in the 2θ range of 15°–27°, marked in the figure, corresponds to the amorphous carbon structure derived from palm fiber. This feature is characteristic of biomass-derived activated carbon and confirms the coexistence of crystalline Fe_3O_4 and amorphous carbon within the composite matrix (H. Sun et al., 2018). The 1:1 composite exhibits intermediate peak intensity and crystallinity, indicating a balanced contribution from both magnetic and dielectric components.

SEM-EDX analysis of Fe_3O_4/C

SEM–EDS analysis revealed that the composite surfaces consist of activated carbon particles with non-uniform sizes and an irregular porous morphology. The formation of open pores was clearly observed, indicating successful activation of the Arenga pinnata (palm fiber)–derived carbon and its integration with iron-sand–derived Fe_3O_4. In several regions, particle

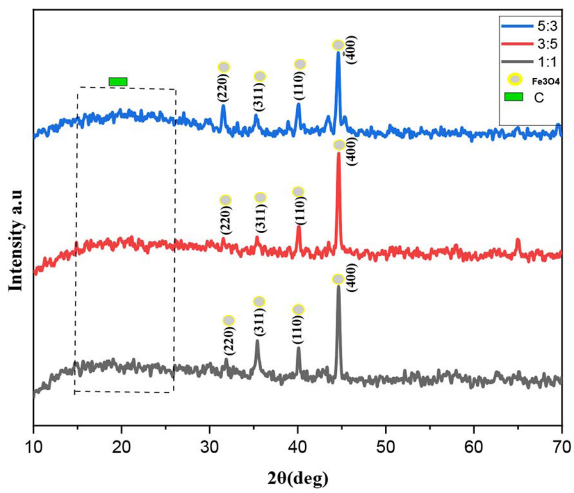

Figure 1. X-ray diffraction pattern

Table 1. Results of calculations of crystal size, lattice parameters, and degree of crystallization

Sample	2θ (deg)	hkl	FWHM (deg)	Lattice parameter (d) (nm)	Crystal size (nm)	Degree of crystallization (%)
1:1	44.64	400	0.33003	2.8530	26.31	74
3:5	44.63	400	0.31391	2.8540	27.77	65
5:3	44.58	400	0.35119	2.8572	26.10	78

agglomeration was evident. This aggregation is attributed to the magnetic dipole–dipole interactions of magnetite particles, which promote interparticle attraction and clustering (Jia et al., 2024). Moreover, Fe_3O_4 particles appear to be partially embedded within the pores and surface cavities of the activated carbon, which can generate new interfacial voids and pore gaps, thereby increasing structural heterogeneity and interfacial contact (Namai et al., 2025; Suryanarayana et al., 2014). Such a porous, heterogeneous microstructure is favorable for microwave absorption because it enhances multiple scattering, interfacial polarization, and dielectric relaxation processes (Sushmita et al., 2019).

EDS results confirm the presence of the expected major elements C, O, and Fe, demonstrating the successful formation of Fe_3O_4/carbon composites, with minor contributions from Si, Al, Na, and Mg likely originating from mineral impurities in natural iron sand and/or residual inorganic species from processing. For the 1:1 composite, the elemental composition was C = 63.5%, O = 15.9%, Fe = 14.3%, Si = 3.1%, Al = 2.0%, Na = 0.5%, Mg = 1.3%, with an average particle size of 0.241 μm. For the 3:5 composite, the composition was C = 55.6%, O = 19.2%, Fe = 12.9%, Si = 5.8%, Al = 3.5%, Na = 3.0%, and an average particle size of 0.216 μm. The 5:3 composite showed C = 73.5%, O = 11.9%, Fe = 8.5%, Si = 1.4%, Na = 1.9%, Al = 1.0%, with a particle size of 0.207 μm (Figure 2).

VNA analysis of Fe_3O_4/C composites

Vector network analyzer (VNA) measurements in the X-band frequency range (8–12 GHz) demonstrate that all Fe_3O_4/activated carbon composites exhibit reflection loss (RL) values lower than −10 dB, confirming their effectiveness as microwave absorbers. As shown in the RL spectra, the 1:1 composite achieved an absorption efficiency of 86% with a minimum RL of −12.39 dB at 11.92 GHz, while the 3:5 composite exhibited the highest absorption performance, reaching 87% with an RL of −12.31 dB at 10.54 GHz. In contrast, the 5:3 composite showed a slightly reduced absorption efficiency of 80%, with an RL of −10.89 dB at 11.92 GHz. According to widely accepted criteria, RL values below −10 dB correspond to more than 90% attenuation of incident electromagnetic waves, indicating effective microwave absorption behavior (Figure 3) (Ashery and Maged, 2022; Houbi et al., 2021; Rani et al., 2021).

The frequency-dependent electromagnetic parameters further support these observations. As illustrated in the permeability (μ) and permittivity (ε) curves, all three composites exhibit similar and overlapping trends, indicating that compositional variation does not significantly alter the intrinsic electromagnetic response within the measured frequency range. Both μ and ε decrease monotonically from approximately 12 to ~2 as frequency increases from 8 to 12 GHz. This behavior is characteristic of Fe_3O_4-based microwave absorbers and reflects the gradual suppression of magnetic domain wall motion, spin rotation, and natural resonance effects at higher frequencies (Zheng et al., 2024). The decline in permittivity with increasing frequency is attributed to the reduced contribution of interfacial polarization (Maxwell–Wagner polarization) and dipolar relaxation processes, which are more effective at lower frequencies (Zhao et al., 2023). Nevertheless, the presence of activated carbon enhances electrical conductivity and promotes dielectric loss through conduction loss and interfacial polarization at Fe_3O_4–carbon interfaces, thereby broadening the effective absorption bandwidth. Meanwhile, the Fe_3O_4 phase provides dominant magnetic loss mechanisms, including natural resonance and eddy current loss, which are essential for microwave attenuation in the X-band (Figure 4) (Negi and Kumar, 2022).

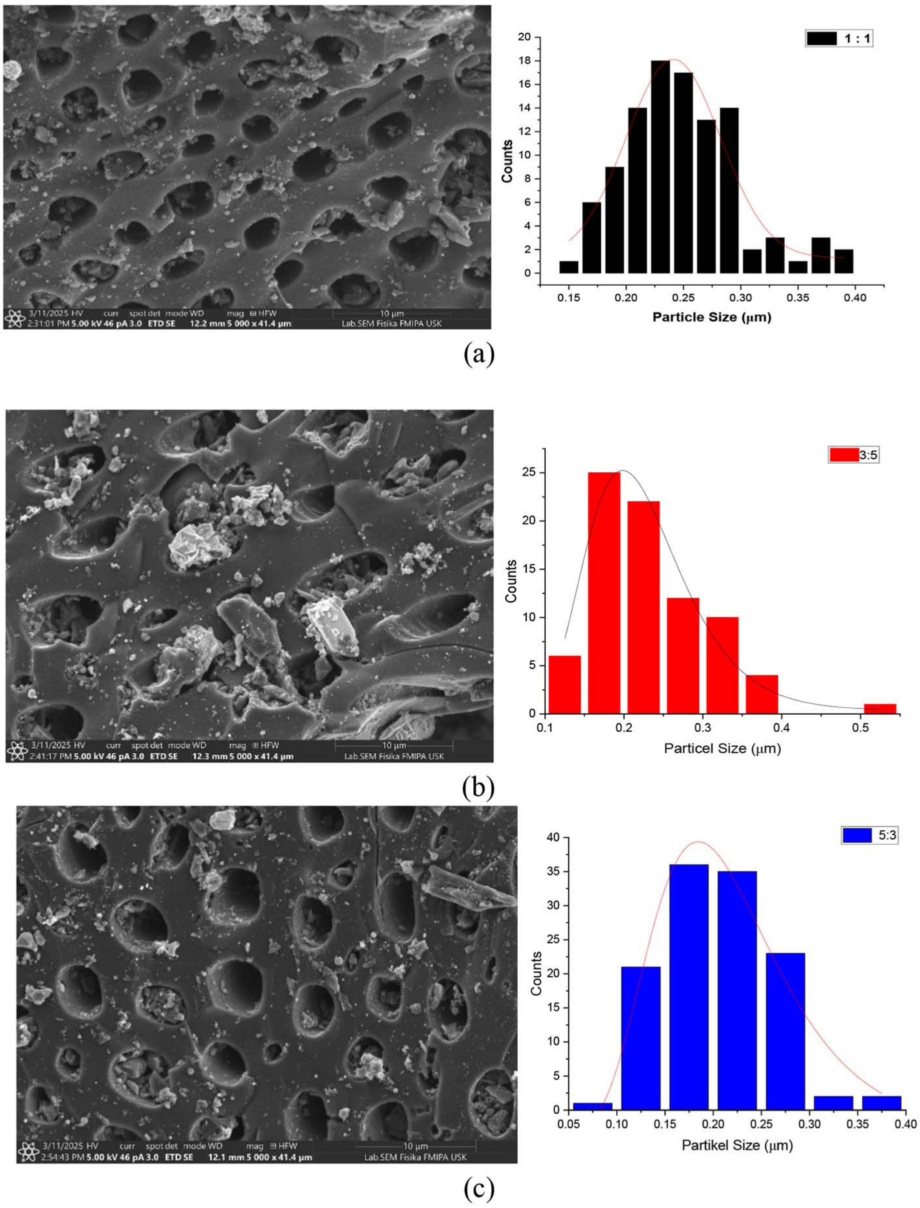

Figure 2. SEM results: Morphology and distribution of particles

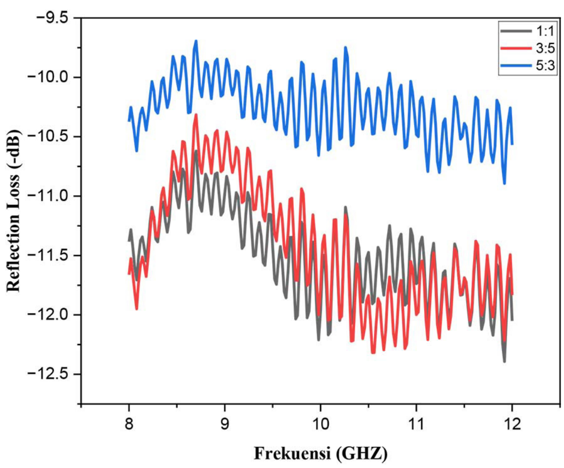

Figure 3. VNA results Loss of reflection from synthesized samples

Importantly, the comparable magnitudes and similar frequency dependence of μ and ε indicate favorable impedance matching, which facilitates efficient penetration of incident electromagnetic waves into the absorber rather than surface reflection. This balanced magnetic–dielectric synergy explains the stable and consistent absorption performance observed across different composition ratios (Zhao et al., 2024). The superior performance of the 3:5 composite can be attributed to an optimal balance between Fe_3O_4-induced magnetic loss and carbon-induced dielectric loss, in agreement with previously reported Fe_3O_4/carbon microwave absorber systems (Lu et al., 2015; Negi, Gupta, et al., 2022; Wei et al., 2024).

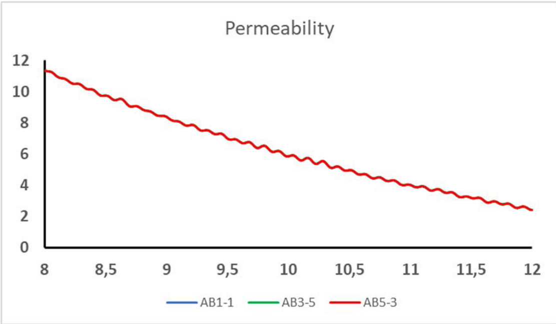

(a)

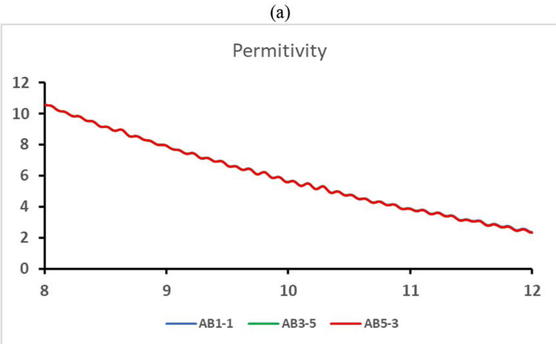

(b)

Figure 4. (a) Permeability curve (μ)
(b) Permeability curve (ε)

CONCLUSIONS

A composite based on Arenga pinnata (ijuk)–derived activated carbon and natural iron sand was successfully synthesized via a coprecipitation-assisted route followed by calcination at 1000 °C. XRD analysis confirmed the formation of a dominant cubic spinel Fe_3O_4 (magnetite) phase with characteristic reflections from the (220), (311), (110), and (400) planes, along with an amorphous carbon phase evidenced by broad diffraction features in the 15°–27° range. SEM–EDX observations revealed porous morphologies composed of agglomerated spherical particles with homogeneous distributions of C, O, and Fe. VNA measurements demonstrated effective microwave attenuation in the X-band, with reflection loss (RL) values below −10 dB, confirming that the synthesized composites function as efficient microwave absorbers. The combined structural, morphological, and electromagnetic results highlight the potential of this sustainable Fe_3O_4/activated carbon system for microwave absorption applications.

Acknowledgments

This research activity is supported through RIIM Kompetisi funding from the Indonesia Endowment Fund for Education Agency, Ministry of Finance of the Republic of Indonesia (Risnov LPDP) and National Research and Innovation Agency of Indonesia according to the contract number: 61/II.7/HK/2024; 45/IV/KS/02/2025 and 4163.1/UN5.4.10.K/PT.01.03/2025. We also thanks to the Universitas Sumatera Utara, Badan Riset dan Inovasi Nasional (BRIN), Universiti Kebangsaan Malaysia for supporting this research activities.

REFERENCES

1. Adrianto, N., Mongkito, V. H. R., Fayanto, S., Anas, M., Eso, R. (2019). Characterization of activated charcoal from sugar palm bunches (*Arengga pinnata* (Wurmb) Merr) and the application as adsorbent lead (Pb), copper (Cu) and chrome (Cr) in solution. *Journal of Physics: Conference Series*. https://doi.org/10.1088/1742-6596/1321/2/022002
2. Al-Mattarneh, H. (2018). Development and characterization of microwave absorber composite material. *International Journal of Engineering and Technology(UAE)*. https://doi.org/10.14419/ijet.v7i3.32.18391
3. Allahkarami, E., Dehghan Monfared, A., Silva, L. F. O., Dotto, G. L. (2022). Lead ferrite-activated carbon magnetic composite for efficient removal of phenol from aqueous solutions: synthesis, characterization, and adsorption studies. *Scientific Reports*. https://doi.org/10.1038/s41598-022-15077-x
4. Ashery, A., Maged, F. A. (2022). Novel structure, electric and dielectric properties of PPy-PANI-GO-MWCNTs composite/MnO_2/Fe_3O_4/n-Si structure. *ECS Journal of Solid State Science and Technology*. https://doi.org/10.1149/2162-8777/ac9f67
5. Chen, J., Ma, L., Wang, X., Wang, Y., Yuan, T., Li, Y. (2025). Fe_3O_4 nanoparticles decorate bamboo clean and sustainable strategies for efficient electromagnetic absorption. *Industrial Crops and Products*. https://doi.org/10.1016/j.indcrop.2025.121737
6. Chitraningrum, N., Marlina, R., Arundina, R. Y., Suryani Togatorop, E. R., Sulistyaningsih, Arisesa, H., Budiman, I., Daud, P., Hamzah, M. (2022). Microwave absorption properties of porous activated carbon-based palm oil empty fruit bunch. *AIP Advances*. https://doi.org/10.1063/5.0128960
7. Chitraningrum, N., Marlina, R., Sutistyaningsih, Arisesa, H., Budiman, I., Daud, P., Septiani, A., Arundina, R. Y., Togatorop, E. R. S. (2024). Preparation and characterization of porous carbon-based oil palm empty fruit bunch as a candidate material for an electromagnetic waves absorber application. *AIP Conference Proceedings*. https://doi.org/10.1063/5.0184349

8. Dipak, P., Tiwari, D. C., Dwivedi, S. K. (2019). Synthesis of polymer blend ferrite composite for microwave absorption at X-Band frequency. *Open Journal of Metal*. https://doi.org/10.4236/ojmetal.2019.94004
9. Elmahaishi, M. F., Azis, R. S., Ismail, I., Muhammad, F. D. (2022). A review on electromagnetic microwave absorption properties: their materials and performance. In *Journal of Materials Research and Technology*. https://doi.org/10.1016/j.jmrt.2022.07.140
10. Fionov, A., Kraev, I., Yurkov, G., Solodilov, V., Zhukov, A., Surgay, A., Kuznetsova, I., Kolesov, V. (2022). Radio-absorbing materials based on polymer composites and their application to solving the problems of electromagnetic compatibility. In *Polymers*. https://doi.org/10.3390/polym14153026
11. Ghigna, T., Zannoni, M., Jones, M. E., Simonetto, A. (2020). Permittivity and permeability of epoxy-magnetite powder composites at microwave frequencies. *Journal of Applied Physics*. https://doi.org/10.1063/1.5128519
12. Houbi, A., Aldashevich, Z. A., Atassi, Y., Bagasharova Telmanovna, Z., Saule, M., Kubanych, K. (2021). Microwave absorbing properties of ferrites and their composites: A review. In *Journal of Magnetism and Magnetic Materials*. https://doi.org/10.1016/j.jmmm.2021.167839
13. Imraan, M., Ilyas, R. A., Norfarhana, A. S., Bangar, S. P., Knight, V. F., Norrrahim, M. N. F. (2023). Sugar palm (*Arenga pinnata*) fibers: new emerging natural fibre and its relevant properties, treatments and potential applications. In *Journal of Materials Research and Technology*. https://doi.org/10.1016/j.jmrt.2023.04.056
14. Izaak, M. P., Gunanto, Y. E., Sitompul, H., Adi, W. A. (2021). Development of magnetic functional materials based on carbon/manganite/ferrite composites for Microwave absorber materials applications. *Jurnal Fisika Dan Aplikasinya*. https://doi.org/10.12962/j24604682.v17i2.8978
15. Jia, Z., Sun, L., Gao, Z., Lan, D. (2024). Modulating magnetic interface layer on porous carbon heterostructures for efficient microwave absorption. *Nano Research*. https://doi.org/10.1007/s12274-024-6939-0
16. Kaur, R., Aul, G. D. (2014). Review on microwave absorbing material using different carbon composites. *International Journal of Engineering Research and Technology*.
17. Li, K., Liu, Z., Wang, Y., Zhang, P., Lin, Z., Fan, S., Xin, T., Du, H., Luo, Z., Wang, C., Yang, W., Yang, J. (2025). Microwave absorption properties and multilayer absorber design of La2FexCo14-xB with easy cone anisotropy. *Journal of Alloys and Compounds*. https://doi.org/10.1016/j.jallcom.2024.177561
18. Li, W., Li, B., Zhao, Y., Wang, Y., Liang, H., Lv, B. (2024). Preparation of an Fe_3O_4 nanoparticle/carbonized hemp fiber composite with superior microwave absorption performance. *ACS Omega*. https://doi.org/10.1021/acsomega.4c07063
19. Liu, Y., Huang, X., Yan, X., Xia, L., Zhang, T., Sun, J., Liu, Y., Zhou, Y. (2023). Pushing the limits of microwave absorption capability of carbon fiber in fabric design based on genetic algorithm. *Journal of Advanced Ceramics*. https://doi.org/10.26599/JAC.2023.9220686
20. Lu, M. M., Cao, M. S., Chen, Y. H., Cao, W. Q., Liu, J., Shi, H. L., Zhang, D. Q., Wang, W. Z., Yuan, J. (2015). Multiscale assembly of grape-like ferroferric oxide and carbon nanotubes: A smart absorber prototype varying temperature to tune intensities. *ACS Applied Materials and Interfaces*. https://doi.org/10.1021/acsami.5b05595
21. Luo, H., Shen, J., Zhang, C. (2019). Retraction notice to Synthesis and microwave absorbing mechanism of two-layer microwave absorbers containing Li 0.35 Zn 0.3 Fe 2.35 O 4 micro-belts and nickel-coated carbon fibers (Composites Part B (2013) 50 (62–66), (S1359836813000231), (10.1016/j.com. In *Composites Part B: Engineering*. https://doi.org/10.1016/j.compositesb.2015.06.017
22. Mahmoodi, M., Aslibeiki, B., Peymanfar, R., Naghshara, H. (2022). Oleaster seed-derived activated carbon/ferrite nanocomposite for microwave absorption in the X-band range. *Frontiers in Materials*. https://doi.org/10.3389/fmats.2022.1088196
23. Meng, L. Y., Ma, M. G., Ji, X. X. (2019). Preparation of Lignin-based Carbon materials and its application as a Sorbent. *Materials*. https://doi.org/10.3390/ma12071111
24. Mohammadifard, A., Allouss, D., Vosoughi, M., Dargahi, A., Moharrami, A. (2022). Synthesis of magnetic Fe_3O_4/activated carbon prepared from banana peel (BPAC@Fe_3O_4) and salvia seed (SSAC@Fe_3O_4) and applications in the adsorption of Basic Blue 41 textile dye from aqueous solutions. *Applied Water Science*. https://doi.org/10.1007/s13201-022-01622-6
25. Namai, A., Yoshikiyo, M., MacDougall, J., Ono, T., Asai, T., Hara, M., Kanai, M., Yoshida, T., Miyamoto, Y., Sakane, K., Kurahashi, S., Nishio, T., Ohkoshi, S. (2025). Ultrathin millimeter-wave–absorbing film for automotive radars based on an epsilon iron oxide/carbon nanotube composite material. *Materials Advances*. https://doi.org/10.1039/d5ma00743g
26. Negi, P., Gupta, A., Singh, M., Kumar, R., Kumar, S., Baskey, H. B., Kumar, A. (2022). Excellent microwave absorbing and electromagnetic shielding performance of grown MWCNT on activated carbon bifunctional composite. *Carbon*. https://doi.org/10.1016/j.carbon.2022.07.024

27. Negi, P., Joshi, S. K., Baskey, H. B., Kumar, S., Mishra, A. K., Kumar, A. (2022). Excellent microwave absorbing performance of biomass-derived activated carbon decorated with in situ-grown $CoFe_2O_4$ nanoparticles. *Materials Advances*. https://doi.org/10.1039/d1ma01116b
28. Negi, P., Kumar, A. (2022). Biomass-derived activated carbon/epoxy composite as microwave absorbing material. *Journal of Electronic Materials*. https://doi.org/10.1007/s11664-022-09558-y
29. Pakniyakan, S., Aslibeiki, B. (2024). Electromagnetic waves absorbing performance of cypress cone derived activated carbon decorated by magnetite nanoparticles. *Diamond and Related Materials*. https://doi.org/10.1016/j.diamond.2024.111324
30. Pattanayak, S. S., Laskar, S. H., Sahoo, S. (2021). Progress on agricultural residue-based microwave absorber: a review and prospects. In *Journal of Materials Science*. https://doi.org/10.1007/s10853-020-05557-8
31. Ramadani, S. S., Zakir, M. (2025). Synthesis and characterization of heterogeneous catalysts from palm fruit shells (*Arenga pinata* Merr.) composited with magnetic nanoparticles Fe_3O_4 (activated …. *The 2nd International Seminar on …*.
32. Rani, B. J., Swathi, S., Yuvakkumar, R., Ravi, G., Kumar, P., Babu, E. S., Alfarraj, S., Alharbi, S. A., Velauthapillai, D. (2021). Solvothermal synthesis of CoMoO4 nanostructures for electrochemical applications. *Journal of Materials Science: Materials in Electronics*. https://doi.org/10.1007/s10854-021-05319-5
33. Rianna, M., Hussain, M. K., Sembiring, T., Guk-Guk, H. P. I. R., Sitorus, K. J., Setiadi, E. A., Tetuko, A. P., Sebayang, P. (2025). Micro-magnetic activity of the fabricated $MnFe_2O_4$ via co-precipitation from natural iron sand. *Science and Technology Indonesia*, *10*(1), 221–227. https://doi.org/10.26554/sti.2025.10.1.221-227
34. Rianna, M., Sembiring, T., Situmorang, M., Kurniawan, C., Tetuko, A. P., Setiadi, E. A., Priyadi, I., Ginting, M., Sebayang, P. (2019). Effect of calcination temperature on Microstructures, magnetic properties, and microwave absorption on BaFe 11.6 Mg 0.2 Al 0.2 O 19 synthesized from natural iron sand. *Case Studies in Thermal Engineering*. https://doi.org/10.1016/j.csite.2019.100393
35. Rianna, M., Setiadi, E. A., Susiani, S., Soehada Sebayang, A. M., Fauzi, M., Hussain, M. K., Yuliana, K., Asri, N. S., Nurdiyansah, L. F., Tetuko, A. P., Sebayang, P. (2023). Enhanced calcination temperatures of SrFe12O19 synthesized by local iron sand from Lombok Island. *Case Studies in Chemical and Environmental Engineering*. https://doi.org/10.1016/j.cscee.2023.100530
36. Salford, L. G., Brun, A. E., Eberhardt, J. L., Malmgren, L., Persson, B. R. R. (2003). Nerve cell damage in mammalian brain after exposure to microwaves from GSM mobile phones. *Environmental Health Perspectives*. https://doi.org/10.1289/ehp.6039
37. Sitepu, E. C., Sembiring, T., Sebayang, K., Sumirat, I., Rianna, M., Marlianto, E., Sukaryo, S. G. (2019). A study of the use of palm fiber and palm shell as a thermal neutron radiation shielding material. *Case Studies in Thermal Engineering*. https://doi.org/10.1016/j.csite.2019.100468
38. Sivaprakash, S., Satheeshkumar, P., Krishna, S. K. (2017). Synthesis & x-ray diffraction characteristic study of agricultural waste activated carbon and AC/Fe_3O_4 – NANO PARTICLES. *Journal of Chemical and Pharmaceutical Sciences*.
39. Sun, H., Lv, Y., Zhang, C., Zuo, X., Li, M., Yue, X., Jiang, Z. (2018). Correction: Materials with low dielectric constant and loss and good thermal properties prepared by introducing perfluorononenyl pendant groups onto poly(ether ether ketone) (RSC Advances (2018) 8 (7753–7760) https://doi.org/10.1039/C7RA13600E). In *RSC Advances*. https://doi.org/10.1039/c8ra90063a
40. Sun, Q., Sun, L., Cai, Y., Ji, T., Zhang, G. (2018). Activated carbon fiber/Fe_3O_4 composite with enhanced electromagnetic wave absorption properties. *RSC Advances*. https://doi.org/10.1039/c8ra05872e
41. Suresha, R., Sachidananda, H. K., Shivamurthy, B., George, G., Parasuram, S. (2025). Structural properties and electromagnetic shielding performance of bidirectional carbon fabric and Fe_2O_3 nano filler reinforced epoxy composites. *RSC Advances*. https://doi.org/10.1039/d5ra06245d
42. Suryanarayana, B., Mouli, K. C., Raghavendra, V., Parvateesam, B. B. (2014). Synthesis and Magnetic studies of Ni-Cu-Zn ferrite Nanocrystals. *Indian Journal of Research in Pharmacy and BiotechnologyOnlinePrint) IJRPB Special Issue*.
43. Sushmita, K., Menon, A. V., Sharma, S., Abhyankar, A. C., Madras, G., Bose, S. (2019). Mechanistic Insight into the nature of dopants in graphene derivatives influencing electromagnetic interference shielding properties in hybrid polymer nanocomposites. *Journal of Physical Chemistry C*. https://doi.org/10.1021/acs.jpcc.8b10999
44. Teber, A., Bansal, R., Unver, I. S., Mehmedi, Z. (2018). The measurement of microwave absorption characteristics of nanocomposites using a coaxial line technique. *International Journal of High Speed Electronics and Systems*. https://doi.org/10.1142/S0129156418400116
45. Wei, H., Dong, K., Men, X., Guo, F., Sun, Z., Kong, L., Zhao, N., Wang, Y., Bai, Y. (2024). Microwave-induced biomass pyrolysis coupled with hydrothermal char composites catalysis to selectively prepare phenols-rich liquid products. *Fuel*. https://doi.org/10.1016/j.fuel.2024.130872

46. Yang, H., Ye, T., Lin, Y., Zhu, J., Wang, F. (2016). Microwave absorbing properties of the ferrite composites based on graphene. *Journal of Alloys and Compounds*. https://doi.org/10.1016/j.jallcom.2016.05.127
47. Ye, W., Li, W., Sun, Q., Yu, J., Gao, Q. (2018). Microwave absorption properties of lightweight and flexible carbon fiber/magnetic particle composites. *RSC Advances*. https://doi.org/10.1039/c8ra05065a
48. Yin, P., Deng, Y., Zhang, L., Li, N., Feng, X., Wang, J., Zhang, Y. (2018). Facile synthesis and microwave absorption investigation of activated carbon@ Fe_3O_4 composites in the low frequency band. *RSC Advances*. https://doi.org/10.1039/c8ra04141e
49. Yin, Z., Du, Y., Yang, L. (2016). Enhanced microwave absorption at low frequency of superparamagnetic Fe_3O_4 single nano-crystals. *Advances in Engineering Research.* https://doi.org/10.2991/aeece-16.2016.47
50. Yusmadi, N. A. N., Azis, R. S., Ismail, I., Katibi, K. K., Alhaji, B. M., Elmahaishi, M. F., Sani, Y., Hongxu, C., Mahmood, M. K. A. (2025). Structural, magnetic, and electromagnetic wave absorption properties of AC/CB–Fe_2O_3 nanocomposites in the Ku-Band. *Journal of Materials Science: Materials in Electronics*. https://doi.org/10.1007/s10854-025-15684-0
51. Zhang, Z., Zhao, H., Gu, W., Yang, L., Zhang, B. (2019). A biomass derived porous carbon for broadband and lightweight microwave absorption. *Scientific Reports*. https://doi.org/10.1038/s41598-019-54104-2
52. Zhao, Y., Li, M., Li, B., Hu, Z. (2024). The honeycomb mesh structure derived from mangosteen shells with excellent microwave absorption properties. *Materials Letters*. https://doi.org/10.1016/j.matlet.2024.136021
53. Zhao, Y., Li, M., Shi, Q., Li, B., Hu, Z., Li, J., Wan, X., Yu, H. (2023). Co/C composites generated from biomass exhibit outstanding electromagnetic wave absorption. *Diamond and Related Materials*. https://doi.org/10.1016/j.diamond.2023.110191
54. Zheng, H., Nan, K., Wang, W., Li, Q., Wang, Y. (2024). Bimetallic nanocubes embedded in biomass-derived porous carbon to construct magnetic/carbon dual-mechanism layered structures for efficient microwave absorption. *Journal of Colloid and Interface Science*. https://doi.org/10.1016/j.jcis.2023.09.121
55. Zhou, J., Lyu, X., Xia, X., Ma, J., Yan, L., Gao, B. (2025). A mini-review of functionalized magnetic Fe_3O_4 nanoparticles: From fundamentals to application. In *Boletin de la Sociedad Espanola de Ceramica y Vidrio*. https://doi.org/10.1016/j.bsecv.2025.100448
56. Zhou, X., Zhang, C., Zhang, M., Feng, A., Qu, S., Zhang, Y., Liu, X., Jia, Z., Wu, G. (2019). Synthesis of Fe_3O_4/carbon foams composites with broadened bandwidth and excellent electromagnetic wave absorption performance. *Composites Part A: Applied Science and Manufacturing*. https://doi.org/10.1016/j.compositesa.2019.105627